

G004

Robust Frequency-domain Multi-parameter Elastic Full Waveform Inversion

R. Brossier* (Joseph Fourier University), S. Operto (CNRS/University of Nice-Sophia-Antipolis/Géoazur) & J. Virieux (Joseph Fourier University)

SUMMARY

Elastic full-waveform inversion is an ill-posed and highly non-linear data-fitting procedure that is sensitive to noise, inaccuracies of the starting model and the definition of multi-parameter classes.

In this study, we investigate the performances of different minimisation functionals, such as the least-square norm (L2), the least-absolute-values norm (L1), and some combinations of both (the Huber and the so-called Hybrid criteria), with an application to a noisy offshore synthetic data set. The four functionals are implemented in a massively parallel, 2D elastic frequency-domain full-waveform inversion algorithm. Results show that, unlike the L2 norm, the L1 norm, the Huber and the Hybrid criteria allow for successful imaging of VP and VS models from noisy data in soft-seabed environment, where the P-to-S waves have a small footprint in the data. The Huber and the Hybrid criteria appear however to be sensitive to a threshold criterion, which requires tedious trial-and-error investigations for reliable estimation. The L1 norm provides a robust alternative to the L2 norm in the framework of efficient frequency-domain full-waveform inversion where a limited number of frequencies are involved in the inversion.

Introduction

Robust quantitative seismic imaging of subsurface parameters is one of the main challenge for oil and gas reservoir characterisation. Full-waveform inversion (FWI) allows to derive high-resolution quantitative models of the subsurface through the exploitation of the full information content of the data (Tarantola, 1987). When applied in the frequency domain, computationally efficient FWI algorithms can be designed by limiting the inversion to a few judiciously chosen discrete frequencies (Sirgue and Pratt, 2004). However, FWI remains an ill-posed and highly non-linear inverse problem that is sensitive to noise, inaccuracies of the starting model and definition of multiparameter classes.

The footprint of the noise in seismic imaging is conventionally mitigated by stacking highly redundant multifold data. However, when the data redundancy is decimated in the framework of efficient frequency-domain FWI, it is essential to assess the sensitivity of inversion to noise. The impact of noise in FWI, when applied to decimated data sets, has been marginally illustrated in the past and the least-squares minimisation formalism remains the most commonly used criterion, although it theoretically suffers from poor robustness in the presence of large isolated and non-Gaussian errors. Other norms can therefore be considered. The least-absolute-values norm (L_1) has been shown to be weakly sensitive to noise in time-domain FWI (Tarantola, 1987; Crase et al., 1990) and in the frequency-domain (Brossier et al., 2009a). Alternative functionals, such as the Huber criterion (Huber, 1973; Guitton and Symes, 2003) and the Hybrid L_1/L_2 criterion (Bube and Langan, 1997) can also be considered. These criteria behave as the L_2 norm for small residuals and as the L_1 norm for large residuals. A threshold controls where the transition between these two different behaviours takes place. However, they assume Gaussian statistics as soon as the L_2 norm is used, leading to the difficult issue of the estimation of the threshold.

In this study, we present applications of 2D elastic frequency-domain FWI to a realistic synthetic data set contaminated by ambient random white noise. We assess the sensitivity of the different functionals to noise when the inversion is applied to few discrete frequencies in the framework of efficient frequency-domain FWI.

Theory

The aim of the FWI is to minimise the data residual vector $\Delta\mathbf{d}$, the difference between the observed data \mathbf{d}_{obs} and the modelled data \mathbf{d}_{calc} . The general form of the minimisation functional \mathcal{C} at iteration k and its gradient \mathcal{G} for FWI can be written as:

$$\mathcal{C}_i^{(k)} = \|\mathbf{S}_d \Delta\mathbf{d}\|_i \quad \mathcal{G}_i^{(k)} = \mathcal{R}\left\{\mathbf{J}' \mathbf{S}_d^\dagger \mathbf{r}^*\right\}, \quad (1)$$

where i is related to the chosen minimisation norm or criterion, \mathbf{S}_d is a data-weighting operator, \mathbf{J} is the Fréchet derivative matrix and \mathbf{r} is the source term of the backpropagated adjoint wavefield that is used in the adjoint-state method for efficient gradient building (Plessix, 2006). Symbols \dagger , t and $*$ denote the adjoint, the transpose and the conjugate operators, respectively. In this study, we consider the L_2 and L_1 norms, and the Huber and the Hybrid criteria. The Figure 1 shows the value of the different functionals and the amplitude of the corresponding adjoint-wavefield sources as a function of the data residual amplitudes. The L_2 norm naturally assigns a high weight to large residuals, which leads to a lack of robustness in the case of incoherent large errors in data. In contrast to the L_2 norm, data residuals are normalised by their amplitudes in the case of the L_1 norm. The Huber and Hybrid criteria follow the L_2 and L_1 behaviours for small and large residuals, respectively. The Huber and Hybrid criteria differ by the shape of the transition between the L_2 and L_1 behaviours and a threshold ϵ controls where the L_2 - L_1 transition takes place.

These criteria are implemented in the massively parallel algorithm described in Brossier et al. (2009c)

Application to the synthetic elastic Valhall model

We assess the four minimisation criteria with the synthetic Valhall model (Figure 2(a)-(b)), which is representative of oil and gas fields in shallow water environment of the North Sea. The main targets are a gas cloud in the large sediment layer and the trapped oil underneath the cap rock of the anticlinal. The acquisition mimics a four-component ocean-bottom-cable survey, with a line of 315 explosive sources positioned 5 m below water surface, and 315 3C sensors on the sea bed at 70 m depth. The geological

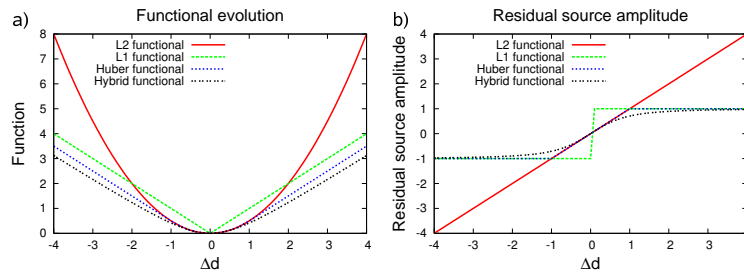


Figure 1 The minimisation criteria (a) and the amplitude of the corresponding adjoint-wavefield source r (b) are plotted as a functions of an unweighted real arithmetic misfit Δd . L_2 , L_1 , and the Huber and Hybrid functionals are plotted with red, green, blue and black lines, respectively.

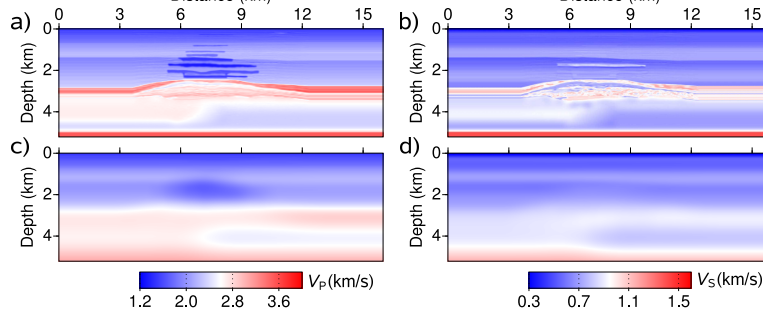


Figure 2 The true synthetic Valhall model for (a) P-wave and (b) S-wave velocities. (c-d) FWI starting models for V_P (c) and V_S (d).

setting leads to a particularly ill-posed problem for S-wave velocity reconstruction, due to the relatively small shear-wave velocity contrast at the sea bed, which prevents recording of significant P-to-S converted waves. Successful inversion requires a multi-step hierarchic strategy as the two-step approach described in Brossier et al. (2009b) for noise-free data:

- 1) In the first step, only the P-wave velocity is reconstructed from the hydrophone data, leading to a quasi-acoustic inversion. This first stage is justified by the fact that the P-to-S converted waves have a minor footprint in the hydrophone component.
- 2) In the second step, the V_P and V_S models are reconstructed simultaneously from the horizontal and vertical components of the geophones.

Five frequencies were inverted successively following the usual multiscale strategy of efficient frequency-domain FWI (2, 3, 4, 5 and 6 Hz). During each frequency inversion, we used 3 time-damping factors ($\gamma=2, 0.33, 0.1 \text{ s}^{-1}$) applied in cascade to the monochromatic data to incorporate progressively later-arriving phases in the inversion. Starting models were built by smoothing the true models with a Gaussian filter (Figure 2(c)-(d)). This smoothing should reasonably mimic the spatial resolution of a velocity model developed by refraction traveltome tomography (Prioux et al., 2009). Ten iterations per damping factor were computed, leading to 30 iterations per frequency inversion. The density is constant and assumed to be known in the inversion. Source signature is estimated during inversion. Two tests were performed, with and without outliers in the data. For both tests, a random uniform white noise was added to the observed data (Figure 3). The signal-to-noise ratio was set to 10 dB, based on the power value of the signal.

FWI Results

For the first test, we considered only the ambient noise. The V_P and V_S models inferred from the four minimisation criteria after the second step of inversion are shown in Figure 4. V_P models are well reconstructed for all functionals, whereas only the robust L_1 norm, the Huber and Hybrid criteria provide acceptable V_S models.

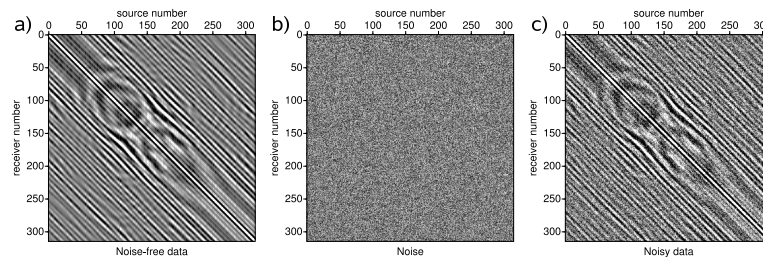


Figure 3 Real part of the 4-Hz frequency-domain data in the source/receiver domain. (a) Noise-free hydrophone data; (b) added random white noise; and (c) resulting contaminated data used for FWI.

In this shallow-water environment with low velocity contrasts at the sea bed, the V_P imaging is more linear than the V_S imaging for two main reasons. Firstly, the larger P-wavelengths are less resolving than their S counterparts, and are therefore less sensitive to the inaccuracies of the starting model in the framework of a multi-scale reconstruction (Brossier et al., 2009c). Secondly, the P-waves dominate the seismic wavefield, whereas the P-to-S waves have a weaker footprint in the data. The limited signature of the S-waves in the data makes the inversion poorly conditioned for the S-wave parameter class, even with noise-free data. Brossier et al. (2009b) have showed how the hierarchical two-step strategy allows to increase the sensitivity of the inversion to the V_S parameter during the second inversion step for a successful reconstruction of the V_S model. However, adding noise to the data still contributes to weaken the sensitivity of FWI to the P-to-S arrivals. In this case, the two-step strategy implemented with the L_2 norm failed to reconstruct the V_S model. In contrast to the L_2 norm, the L_1 norm, the Huber and the Hybrid criteria successfully converge towards acceptable V_S models by mitigating the impact of the noise in the reconstruction.

In a second test, we have introduced outliers into the data: large errors (i.e., the noise was locally multiplied by 20) were introduced randomly in one trace out of a hundred, to simulate a poorly preprocessed data set. The V_P models obtained after the first inversion step with the four functionals are shown in Figure 5. The L_1 norm, and the Huber and Hybrid criteria provide accurate V_P models, whereas the inversion rapidly converges towards a local minimum when the L_2 norm is used.

As expected, the L_2 norm fails to successfully reconstruct the V_P model in the presence of high-amplitude isolated errors. Indeed, the L_2 norm amplifies the weight of the high-amplitude residuals during inversion, hence causing divergence of the optimisation if the residuals do not correspond to useful seismic arrivals. The L_1 norm, as well as the Huber and Hybrid criteria, shows stable behaviour for V_P imaging in this unfavourable context, because the isolated high-amplitude outliers have a negligible contribution in these functionals.

Conclusion

Application of elastic FWI to noisy offshore data shows the strong sensitivity of the L_2 norm to non-Gaussian errors in the data, when decimated discrete frequencies are considered in FWI. The marginally used L_1 norm appears to be weakly sensitive to noise even in the presence of outliers, and provides stable results for FWI applications. Alternative functionals, such as the Huber and Hybrid criteria, which combine the L_1 and L_2 norms, provide stable results if the threshold controlling the transition between the two behaviours is well chosen. The judicious estimation of this threshold by trial-and-error is however a clear drawback of these criteria. More automatic functionals, such as the L_1 norm, should therefore be recommended for inversion of field data. The L_1 norm reveals an interesting alternative to the L_2 norm, especially when decimated data-sets are processed by efficient frequency-domain FWI.

Acknowledgements

This study has been funded by the SEISCOPE consortium <http://seiscope.oca.eu>, sponsored by BP, CGG-VERITAS, EXXON-MOBIL, SHELL and TOTAL, and by ANR under project ANR-05-NT05-2-42427. Access to the high-performance computing facilities of MESOCENTRE SIGAMM (OCA) and IDRIS (CNRS) computer centres provided the required computer resources.

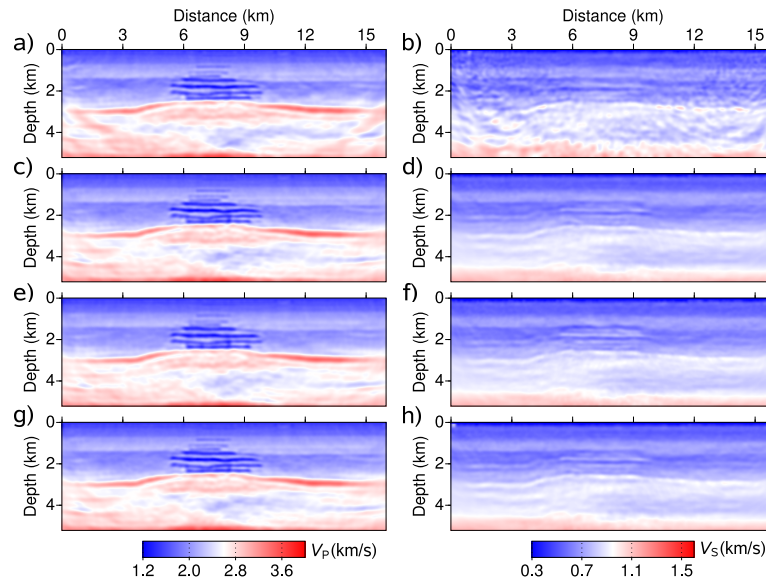


Figure 4 Reconstructed V_P (left panels) and V_S (right panels) models for the first test with the ambient noisy data. (a-b) L_2 norm; (c-d) L_1 norm; (e-f) Huber criterion; and (g-h) Hybrid criterion.

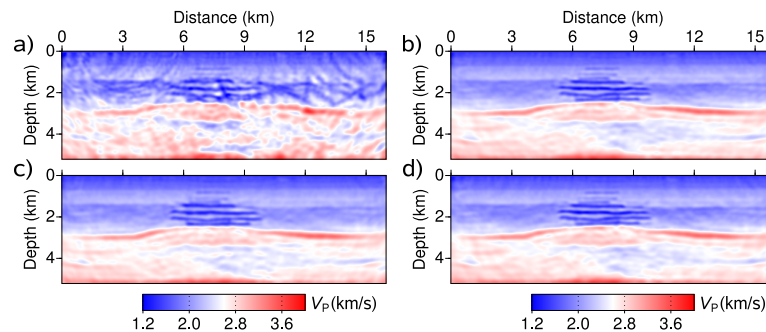


Figure 5 Reconstructed V_P models for the second test with the noisy data containing outliers. (a) L_2 norm; (b) L_1 norm; (c) Huber criterion; and (d) Hybrid criterion.

References

- Brossier, R., Operto, S. and Virieux, J. [2009a] Robust frequency-domain full-waveform inversion using the l_1 norm. *Geophysical Research Letters*, **36**, L20310, doi:10.1029/2009GL039458.
- Brossier, R., Operto, S. and Virieux, J. [2009b] Two-dimensional seismic imaging of the Valhall model from synthetic OBC data by frequency-domain elastic full-waveform inversion. *SEG Technical Program Expanded Abstracts*, **28**(1), 2293–2297.
- Brossier, R., Operto, S. and Virieux, J. [2009c] Seismic imaging of complex onshore structures by 2D elastic frequency-domain full-waveform inversion. *Geophysics*, **74**(6), WCC63–WCC76, doi:10.1190/1.3215771.
- Bube, K.P. and Langan, R.T. [1997] Hybrid l_1/l_2 minimization with applications to tomography. *Geophysics*, **62**(4), 1183–1195, doi:10.1190/1.1444219.
- Cruse, E., Pica, A., Noble, M., McDonald, J. and Tarantola, A. [1990] Robust elastic non-linear waveform inversion: application to real data. *Geophysics*, **55**, 527–538.
- Guitton, A. and Symes, W.W. [2003] Robust inversion of seismic data using the Huber norm. *Geophysics*, **68**(4), 1310–1319, doi:10.1190/1.1598124.
- Huber, P.J. [1973] Robust regression: Asymptotics, conjectures, and Monte Carlo. *Ann. Statist.*, **1**(5), 799–821.
- Plessix, R.E. [2006] A review of the adjoint-state method for computing the gradient of a functional with geophysical applications. *Geophysical Journal International*, **167**(2), 495–503.
- Prieux, V., Operto, S., Brossier, R. and Virieux, J. [2009] Application of acoustic full waveform inversion to the synthetic Valhall model. *SEG Technical Program Expanded Abstracts*, **28**(1), 2268–2272.
- Sirgue, L. and Pratt, R.G. [2004] Efficient waveform inversion and imaging : a strategy for selecting temporal frequencies. *Geophysics*, **69**(1), 231–248.
- Tarantola, A. [1987] *Inverse problem theory: methods for data fitting and model parameter estimation*. Elsevier, New York.